05

Experimental investigation and modeling of the generation conditions of a distributed feedback laser based on erbium-doped active optical fiber

© Ya.D. Moor, A.V. Kulikov, A.N. Arzhanenkova, K.A. Konnov, G.P. Miroshnichenko

ITMO University,
St. Petersburg, Russia

e-mail: moorID@itmo.ru

Received November 01, 2025
Revised January 27, 2026
Accepted February 04, 2026

This paper presents the results of an experimental investigation and mathematical modeling of the lasing conditions in a distributed-feedback fiber laser based on a fiber Bragg grating (FBG) inscribed in erbium-doped active optical fiber. FBGs with lengths of 50, 60, 65, and 70 mm were studied. The influence of the optical-fiber parameters on the stability and characteristics of laser emission was investigated. The results show that stable single-frequency lasing requires a sufficient gain parameter of the active medium, as confirmed by experiments with FiberCore I-25, I-12, and M-12 optical fibers. Splitting of the lasing spectrum for an FBG length of 70 mm was observed experimentally and explained using the developed mathematical model. Modeling based on a system of coupled-mode equations that incorporates spontaneous-emission noise demonstrates that the introduction of a small chirp ($\xi = 4.3 \cdot 10^{-3}$ nm/cm) into the fiber Bragg grating structure stabilizes the spectral peak of amplified spontaneous emission (ASE), which represents the initial stage of laser generation, similarly to the effect of introducing a π-phase shift. The results are important for the development of highly stable single-frequency distributed feedback lasers employed in high-precision sensing systems and optical communications.

Keywords: distributed feedback (DFB) laser, fiber Bragg grating (FBG), erbium-doped optical fiber, laser generation, phase-mask scanning technique, mathematical modeling of amplified spontaneous emission (ASE).

DOI: 10.61011/0000000000

Introduction

The use of single-frequency fiber lasers, the radiation of which contains only one longitudinal mode may be relevant for high-frequency measurement systems for detecting vibration effects and acoustic signals, which are used in marine and terrestrial seismic exploration, as well as monitoring of mineral deposits [1]. The narrow generation line and low level of phase noise of a fiber quasi-monochromatic source are attractive for creating sensors of physical quantities. These properties are possessed by distributed feedback lasers (DFB lasers) based on fiber Bragg gratings (FBG) [2].

Fiber-optic DFB lasers are widely used in optical communication lines and sensor systems due to their compactness in terms of assembly into the final product [3,4]. The resonator of such lasers consists of a FBG, usually with π-phase shift, induced directly into an active optical fiber doped with rare earth elements (Er, Yb, Tm, Ho) [5]. Unlike a fiber laser with a distributed Bragg reflector, which consists of two passive FBGs with an active fiber section between them, the DFB laser manufacturing process proposed in this paper is more technologically advanced, since it does not require additional π-phase shift in the FBG, as in Ref. [5], and the connection of different types of fibers, as in the case of two passive FBGs. At the same time, to create a DFB laser, it is necessary to select the parameters of the optical fiber (OF) in such a way as to ensure stable laser generation of the active optical fiber, which is the purpose of this study.

Experiment and analysis of experimental data

A distributed feedback laser in OF FiberCore I-25(980/125) [6] (parameters of the laser: pump wavelength 980 nm, numerical aperture 0.23−0.26, absorption at wavelength 1531 nm 35−45 dB/m) was created by inducing FBG with lengths of 50, 60, 65 and 70 mm by the phase mask method using a KrF excimer laser Coherent COMPexPro 102F (central wavelength 248 nm), an interference-coated mirror at 248 nm, a high-precision linear translator with a stroke of 100 mm, a phase mask (PM) Ibsen Photonics, optimized for ± 1 diffraction order (FM parameters: period 1071.5 nm, diffraction grating size 70×10 mm). The laser beam moved along a stationary PM and OF, inducing a FBG into an optical fiber with a length greater than the geometric size of the beam (20×8 mm). This recording technology was previously presented in Ref. [7] and made it possible to induce a FBG up to 70 mm in length, doped with erbium ions with a

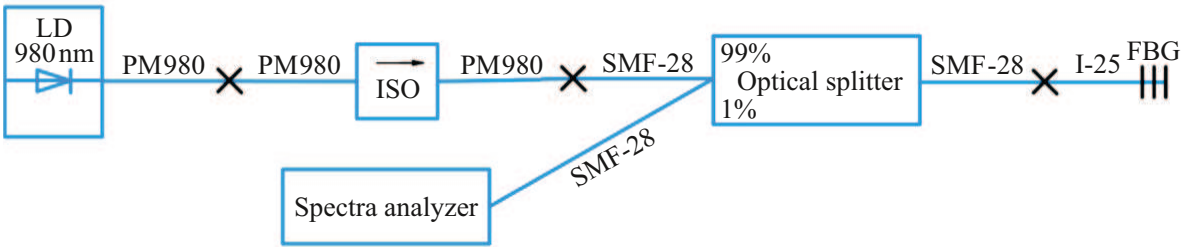


Figure 1. A fiber-optic laser radiation generation circuit with distributed feedback based on a single FBG with a constant period of refractive index modulation.

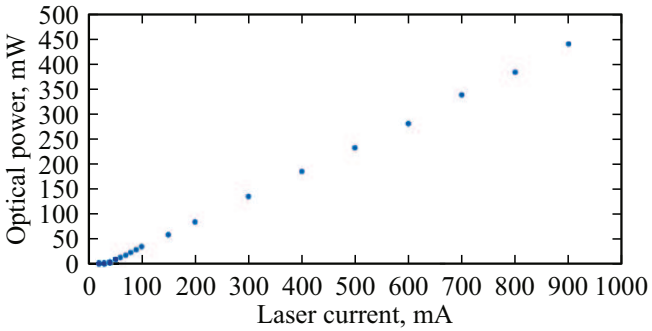


Figure 2. Watt-ampere characteristic of the Laser Enterprise II-VI UM96Z460-76 pump diode, obtained experimentally.

half-height reflection spectrum of about 40−50 pm and a reflection coefficient of more than 99 %.

A fiber-optic scheme shown in Fig. 1 was used to generate optical radiation in the formed FBG-based DFB laser. Radiation from a pumped laser diode (Laser Enterprise II-VI UM96Z460-76) with a wavelength of 976 nm (LD) (preliminary measurements to determine the watt-ampere characteristic are shown in Fig. 2) through a fiber-optic insulator and an optical coupler fell on the FBG with a constant period of refractive index modulation. The radiation generated by a FBG-based DFB laser was directed through an optical coupler to an optical radiation analyzer (Yokogawa AQ6370*C*).

A study of the dependence of the central wavelength of the DFB laser generation on the radiation power of a laser diode, which was studied in detail earlier in jcite8, showed that the spectrum width of the DFB laser generation at the 3 dB level is significantly narrower than the spectrum width of this FBG (Fig. 3). Therefore, the use of high-performance single-frequency fiber lasers based on FBG can significantly increase the accuracy of phase shift detection.

Fig. 3 shows the spectral distribution of the amplified spontaneous emission (ASE) of a fiber-optic laser and the reflection spectrum of the FBG, obtained on the basis of mathematical calculations (the model description will be described below), for a FBG with a length of 65 mm, with a wavelength-independent gain $\kappa = 1.5 \cdot 10^{-4}$ db/μm, depth effective refractive index modulations $\Delta n_{ef} = 0.78 \cdot 10^{-4}$, resonant wavelength $\lambda_{res} = 1.5515\,\mu$m, $n_{ef} = 1.45$ — effective mode refractive index, apodization parameter $\gamma = 0.45$, chirping parameter $\xi = 4.3 \cdot 10^{-3}$ nm/cm. The calculation was performed for the FBG, which is divided into $K = 100$segments of random length, spontaneous noise modules are randomly selected according to a uniform distribution in the range from 0 to 0.03 arbitrary units, spontaneous noise phases are selected according to a uniform distribution in the range from 0 to 2π randomly. The amplitudes and phases of spontaneous noise are considered to be independent of the wavelength.

The calculated peak of the spectral distribution of the amplified spontaneous radiation of a fiber laser is visible (in relative units) in the spectrum of the experimental generation study, the width of the amplification spectrum is about 5 pm. The intensity depends on the realization of spontaneous noise. At wavelengths in the short-wavelength region, a change in the intensity of the ASE spectrum is observed from the calculated peak of the spectral distribution of the amplified spontaneous radiation of the fiber DFB laser, associated with an increase in noise uniform in wavelength.

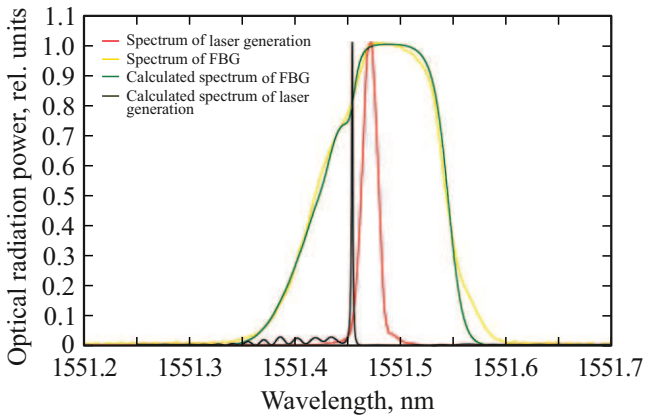


Figure 3. The measured reflection spectra of the FBG (yellow), generation of a DFB laser based on the FBG with a length of 65 mm at a pump current of 600 mA (red) and mathematically calculated reflection spectra of the FBG (green) and the spectral distribution of the amplified spontaneous radiation of the fiber DFB laser (black).

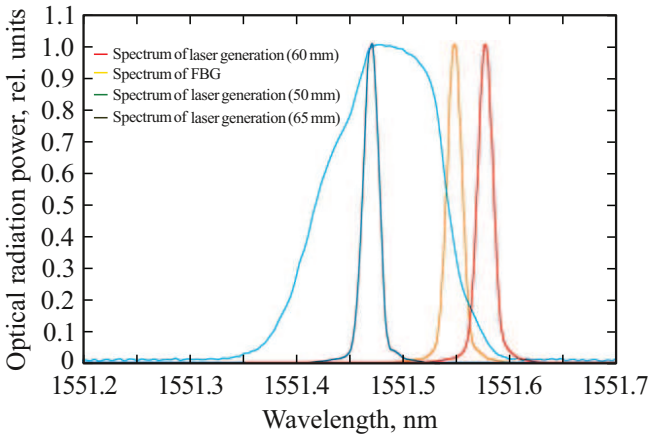


Figure 4. The emission spectra of a FBG-based DFB laser with lengths of 50 (red), 60 (orange) and 65 mm (blue) at a pump current of 600 mA, normalized to the maximum radiation power value blue line — 65 mm long FBG experimental reflection spectrum.

Fig. 3 shows the spectral distribution of the amplified spontaneous radiation of a fiber DFB laser, normalized to the maximum value, calculated according to the model presented below, in a linear approximation, when the gain does not depend on the ASE intensity (a slight excess of the generation threshold). This is the initial stage of DFB laser generation, in which, due to the selective properties of the FBG, generation modes begin to form in the spectral regions located at the boundaries of the FBG reflection spectrum, where optimal conditions for feedback are provided

This is an unobvious property of the FBG interacting with spontaneous noise, since the FBG performs two functions peculiar to the resonator: it creates a distributed feedback that lengthens the path of photons in the active medium, and it is a selective element that selects waves of certain wavelengths, from which the modes of generation of the DFB laser are further formed.

It should be noted that the reflection spectra of the FBG and the spectral distribution values of the amplified spontaneous emission of a fiber DFB laser are calculated for the FBG with the addition of a small chirping coefficient $\xi = 4.3 \cdot 10^{-3}$ nm/cm. As the calculation shows, the location of the peak along the wavelength of the ASE does not depend on the realization of spontaneous noise. It was noted in Ref. [3–5] that stabilization of the wavelength of laser generation is possible with the introduction of π-shift of phase in the middle of the FBG. Our calculations have demonstrated that the introduction of the chirping effect also stabilizes the wavelength of laser generation.

It is worth noting that the experimental spectrum of DFB laser generation (Fig. 3) is wider than the calculated value of the spectral distribution of the amplified spontaneous radiation of a fiber DFB laser. This key discrepancy is directly related to the simplifications embedded in the mathematical model. In our calculation, we deliberately did not take into account nonlinear effects (first of all, saturation of the gain coefficient with the intensity of the ASE), which inevitably occur in a real experiment when the intensity thresholds are reached and exceeded. It is the saturation effect that leads to the broadening of the generated spectrum and its transformation.

According to the results of the study, at a wavelength of 70 mm and a pump current of 600 mA, spectrum splitting was observed (Fig. 5), while for wavelengths of 50, 60, and 65 mm, spectrum splitting of laser generation was not observed (Fig. 4).

This experiment (Fig. 4) was carried out with a 65 mm long FBG, the length of which was reduced due to the chipping of the FBG. The free end was placed in an immersion gel to eliminate back reflections. As the length decreased, the spectrum of laser generation shifted to the long-wavelength region, which is presumably due to thermal effects resulting from the long duration of the experiment.

The experiment for a 70 mm long FBG revealed splitting of the laser generation spectrum at pumping currents from 600 to 900 mA (Fig. 5).

The observed effect of spectrum splitting is visible in calculations based on the developed mathematical model (Fig. 6). The peaks of the spectral distribution of the amplified spontaneous radiation of a fiber-optic laser are formed at the boundaries of the reflection spectrum of the FBG, in the central region of the spectrum a zone is formed in which there is no laser generation (the radiation is captured by the FBG). There is no amplification of spontaneous radiation in the regions of the spectrum beyond the reflection spectrum of the FBG, where there is no feedback.

Fig. 6 shows the calculation of the spectral distribution of the amplified spontaneous radiation of a FBG-based fiber DFB laser (relative values) for a FBG with zero chirping effect. The calculation is performed for the parameters $\kappa = 1.5 \cdot 10^{-4}$ dB/μm, $\Delta n_{ef} = 0.65 \cdot 10^{-4}$, $\xi = 0$, $\gamma = 0.45$, $\lambda_{res} = 1.55158\,\mu$m, $n_{ef} = 1.45$. In this case, a spectrum with one or two peaks is possible; this means that the wavelength of the laser generation is unstable. A critical parameter for the appearance of laser generation of a DFB laser is the gain parameter (the difference between the gain and absorption coefficients for a given section of the optical fiber) of the active component. According to the results of the study, it was found that with the same parameters of FBG recording, laser radiation generation is observed in the active OF doped with erbium ions FiberCore I-25(980/125) [6], and there is no laser generation in the optical fiber FiberCore I-12(980/125) [9] and FiberCore M-12(980/125) [10]. The gain parameter at the wavelength of the Bragg resonance 1551.5 nm was calculated in a specialized FiberCore GainMaster production environment and was $k = 0.238 \cdot 10^{-4}$ dB/μm

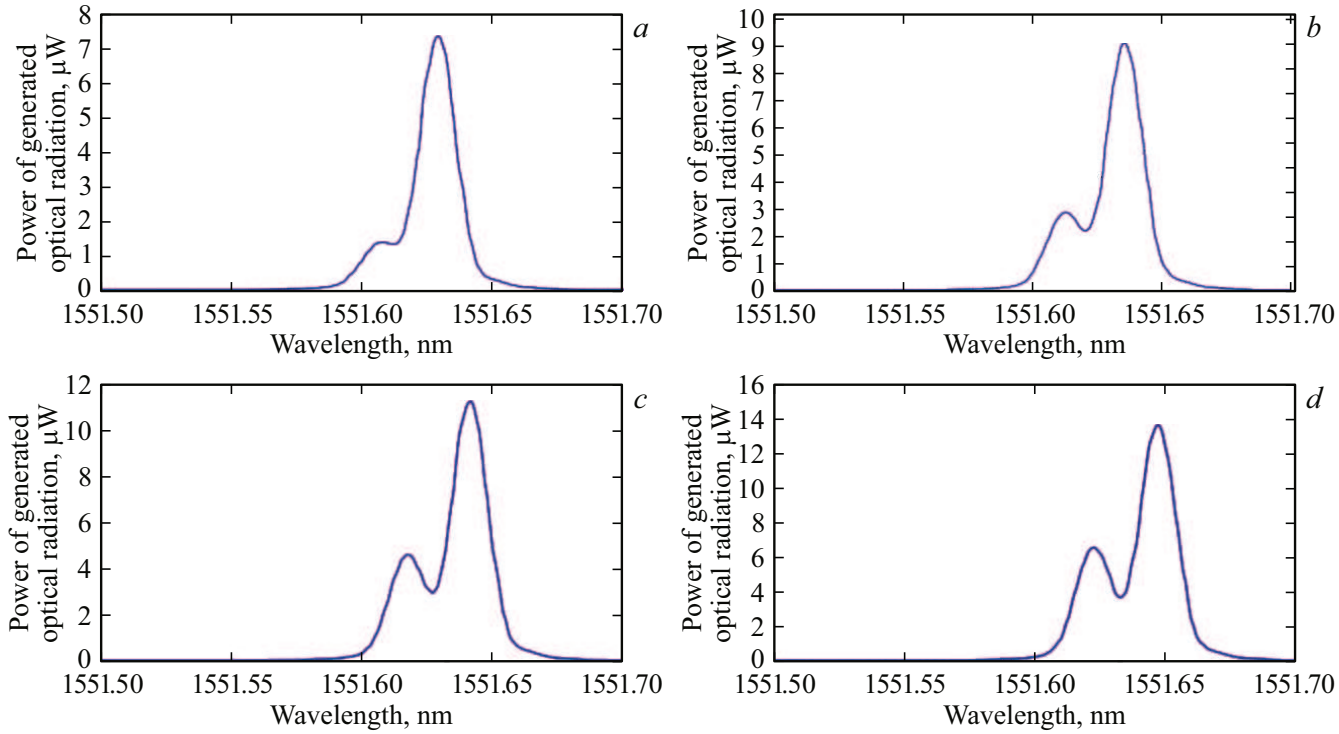


Figure 5. Distributed feedback laser radiation spectra based on FBG with a length of 70 mm at a pump current from 600 to 900 mA, where *a* — 600,mA, *b* — 700,mA, *c* — 800 mA, *d* — 900 mA.

for FiberCore I-25, $k = 0.110 \cdot 10^{-4}$ dB/μm for FiberCore I-12, $k = 0.138 \cdot 10^{-4}$ dB/μm for FiberCore M-12. Thus, in order to efficiently generate the laser radiation of a FBG-based DFB laser, it is necessary to take into account the optical fiber amplification parameter.

Simulation of the spectral intensity of amplified spontaneous radiation for an intensity-independent gain factor. System of equations and its solution

When creating a model for the generation of a DFB laser, it is necessary to take into account the interaction of counter modes on the FBG, the gain factor and the seed spontaneous noise. The proposed model investigates the amplification of chaotic spontaneous radiation under the action of an inverted medium and selective FBG in the approximation of a constant and wavelength-independent gain factor. The electric field of two counter-directional waveguide modes in the FBG (in the scalar single-mode approximation) is written as:

$$E(\rho, \varphi, z, t) = a(z)F_a(\rho, \varphi)\exp\big(i(\omega t - \beta z)\big) + b(z)F_b(\rho, \varphi)\exp\big(i(\omega t + \beta z)\big), \quad (1)$$

where $F_a(\rho, \varphi), F_b(\rho, \varphi)$ — the forward and reverse transverse main modes of an ideal optical fiber; ω, β — the frequency and propagation constant of the counter-directional modes in the FBG; z — the longitudinal coordinate; $a(z), b(z)$ — the amplitudes of the forward and reverse propagating modes, depending on the longitudinal coordinate z; ρ, φ — transverse cylindrical coordinates.

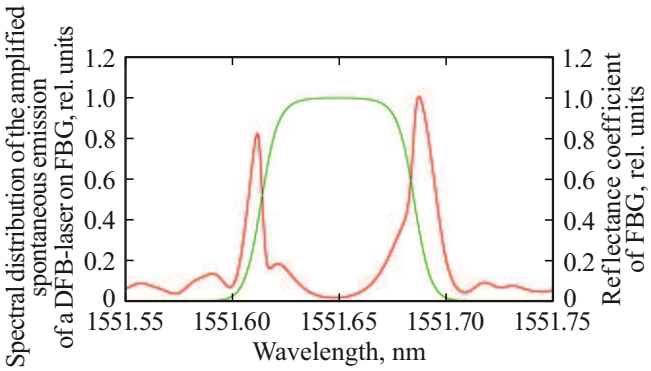


Figure 6. The calculated spectral distribution of the reflection coefficient of a 65 mm-long FBG (green) and the spectral distribution of the amplified spontaneous radiation of a fiber DFB laser based on it (red) obtained in the model.

Let's substitute the equation (1) in the wave equation, we obtain a system of Helmholtz differential equations for $a(z), b(z)$ amplitudes, in the approximation of slow wave

envelopes, by analogy with Ref. [11–13],

$$\begin{cases} \frac{da(z)}{dz} = \left(-i\,\frac{2\pi\Delta n_{ef}}{\lambda}\,Ap(z) + \kappa\right)a(z) - i\,\frac{\pi\Delta n_{ef}}{\lambda}\,Ap(z) \\ \quad \times \exp\left(i\left(\Delta\beta(\lambda)z - 2\pi\xi(\frac{z}{\Lambda})^2\right)\right)b(z), \\ \frac{db(z)}{dz} = i\,\frac{\pi\Delta n_{ef}}{\lambda}\,Ap(z)\exp\left(-i\left(\Delta\beta(\lambda)z - 2\pi\xi(\frac{z}{\Lambda})^2\right)\right) \\ \quad \times a(z) + \left(i\,\frac{2\pi\Delta n_{ef}}{\Lambda}\,Ap(z) - \kappa\right)b(z), \end{cases} \tag{2}$$

where $a(z)$ and $b(z)$ describe the amplitudes of two opposing (forward and reverse) modes in the waveguide, λ — wavelength of propagating radiation, Δn_{ef} — depth of modulation of the effective refractive index of the fiber core, $Ap(z) = \exp\left(-\left(\frac{z-L/2}{\gamma L/2}\right)^2\right)$ — apodization function, κ — gain parameter (taking into account amplification and absorption optical fiber), $\Delta\beta(\lambda) = \left(4\pi \cdot n_{ef}/\lambda - 2\pi/\Lambda\right)$ — phase synchronism factor, $\Lambda = \lambda_{res}/2 \cdot n_{ef}$ — FBG period, n_{ef} — effective mode refractive index, λ_{res} — resonant FBG wavelength, ξ — chirping parameter, γ — Gaussian apodization parameter.

Solving the equation (2) is performed using the $\hat{M}(z)$ development matrix using the Cauchy method based on the initial data $a(0)$, $b(0)$, equation (3):

$$\begin{pmatrix} a(z) \\ b(z) \end{pmatrix} = \hat{M}(z)\begin{pmatrix} a(0) \\ b(0) \end{pmatrix}, \tag{3}$$

where the beginning of the FBG is at $z = 0$.

The development matrix is found by numerically solving the system of equations (2) using the second-order Runge-Kutta method. The modeled DFB laser does not have a conventiona mirror resonator. In our case, the distributed feedback necessary for generation occurs due to multiple re-reflections of waves on the FBG refractive index modulation. The synchronization conditions depend on the wavelength. Spontaneous seed noise is necessary for the occurrence of laser generation in the semiclassical description. We propose a model for introducing random spontaneous noise into equations (2). Let's split the FBG into K segments numbered $1 \le k \le K$. Let's denote the initial coordinate of the k-th segment by z_{k-1}, the final coordinate by z_k, and set in each point $z_0, z_1, \ldots z_k$ two random, evenly distributed in modulus and phase complex numbers $\varepsilon_k^a = r_k^a \cdot \exp(i\varphi_k^a)$, $\varepsilon_k^b = r_k^b \cdot \exp(i\varphi_k^b)$, meaning random amplitudes of forward and reverse waves of spontaneous noise. Let us denote ε_0^a —the incident spontaneous wave at the initial point of the FBG, $b(z_0)$ — the amplitude of the reflected FBG wave at the initial reference point of the FBG. Then, according to equation (3), the solution of equation (2) to determine the amplitudes of the waves after the first segment, they will be written as:

$$\begin{pmatrix} a(z_1) \\ b(z_1) \end{pmatrix} = \hat{M}(z_1) \cdot \begin{pmatrix} \varepsilon_0^a \\ b(z_0) \end{pmatrix}.$$

Hereafter, the development matrices of the k-th segment are designated $\hat{M}(z_k)$. At the z_1 point, we add the amplitudes of spontaneous noise $\begin{pmatrix} \varepsilon_1^a \\ \varepsilon_1^b \end{pmatrix}$ to the amplitudes of $\begin{pmatrix} a(z_1) \\ b(z_1) \end{pmatrix}$.

Then we get the field at the output of the second segment in the form:

$$\begin{pmatrix} a(z_2) \\ b(z_2) \end{pmatrix} = \hat{M}(z_2)\hat{M}(z_1)\begin{pmatrix} \varepsilon_0^a \\ b(z_0) \end{pmatrix} + \hat{M}(z_2)\begin{pmatrix} \varepsilon_1^a \\ \varepsilon_1^b \end{pmatrix}.$$

Then we should continue by analogy to the last segment of the FBG. Let's introduce the sequence of $\hat{W}(q)$ $q = 0, 1, \ldots K-1$ matrices using the formula

$$\hat{W}(q) = \prod_{k=0}^{K-1-q} \hat{M}(z_{K-k}). \tag{4}$$

The amplitude of spontaneous noise ε_K^b decreases from theend segment of the reference to the FBG, as a result, it should be taken intoaccount that

$$b(z_K) = \varepsilon_K^b. \tag{5}$$

From the equations (4) and (5) we obtain the amplitude of the ASE wave $a(z_K)$ propagating from the initial to the final point of the grid and the amplitude of the ASE wave $b(z_0)$ propagating from the end point of the grid towards the initial point

$$\begin{cases} b(z_0) = \frac{\varepsilon_K^b - \Sigma_{q=1}^{K-1}(\hat{W}(q)_{1,0}\varepsilon_q^a + \hat{W}(q)_{1,1}\varepsilon_q^b) - \hat{W}(0)_{1,0}\varepsilon_0^a}{\hat{W}(0)_{1,1}} \\ a(z_K) = \Sigma_{q=1}^{K-1}(\hat{W}(q)_{0,0}\varepsilon_q^a + \hat{W}(q)_{0,1}\varepsilon_q^b) \\ \quad + \hat{W}(0)_{0,0}\varepsilon_0^a + \hat{W}(0)_{0,1}b(z_0) \end{cases}.$$

The spectral distribution of the amplified spontaneous radiation of a FBG-based fiber DFB laser emanating from the FBG end point is determined by the formula: $I_a(\lambda) = |a(z_K)|^2$, the spectral distribution of the ASE emanating from the starting point of the FBG is determined by the formula: $I_b(\lambda) = |b(z_0)|^2$. Due to the linearity of the problem, the calculation is performed independently for each wavelength, the noise modules and phases are selected randomly. For further analysis of the results, we will consider the ASE coming from the starting point of the FBG. The radiation intensity depends on the implementation of spontaneous noise and the gain parameter, so the result was normalized to the maximum value and given in relative units. This is done for a qualitative comparison of the spectral shape within the framework of this linear model, where the absolute intensity values do not have a fundamental physical meaning, but the shape and position of the spectral peaks are important.

In conclusion, we note that the mathematical model of laser generation with distributed feedback adopted in the work is linear in the field and uses a gain independent of time and field. It is assumed that such a mathematical model can describe the spectral intensity of enhanced spontaneous radiation, the moment of the appearance of laser generation, when the population inversion of erbium levels does not begin to deplete from the ASE intensity. Calculations show that an apodized and chirped fiber Bragg grating recorded in an active optical fiber doped with

erbium ions plays the role of a selective element, organizing narrow-spectral radiation modes from spontaneous noise. The waves of the spectral distribution of the amplified spontaneous radiation are re-reflected by a change in the FBG refractive index modulation, which leads to an increase in the path length in the inverted region. The spectrum of modes of the spectral distribution of the ASE turns out to be narrow and concentrates in areas at the edges of the reflection spectrum of the FBG. At wavelengths near the central wavelength of the Bragg resonance, a band gap is formed for generation. Generation does not occur in the short-wave and long-wave reflection regions of the FBG. In order to describe the nonlinear stage of DFB laser generation (after reaching the threshold value of intensity and establishing the laser generation mode), it is necessary, as is known, to solve the associated system of equations of matter and field in the presence of a FBG, as a kind of resonator, taking into account the saturation of the population inversion. This difficult task has not been set in this paper. It can be assumed that some broadening of the spectrum of mode generation is associated with the effect of saturation inversion. Obviously, our simplified model can only claim a qualitative comparison with expiremental data.

Conclusions

The model presented by us is an effective tool for a qualitative explanation and prediction of the wavelength at which laser generation occurs in a FBG-based DFB laser induced in an active optical fiber. It allows determining the areas of the reflection spectrum in which there is no generation and the wavelengths at which laser generation occurs.

It is necessary to calculate the optical fiber gain parameter in order to determine the possibility of laser generation to manufacture a distributed feedback laser based on an active optical fiber doped with erbium ions with an induced fiber Bragg grating with a constant refractive index modulation period of more than 40 mm.

For an effective implementation of a distributed feedback laser, it is important to choose an optical fiber with the appropriate gain parameter. The results of experimental work and computer modeling have confirmed that when using optical fibers with a gain parameter greater than $k = 0.2 \cdot 10^{-4}\,\mathrm{dB}/\mu\mathrm{m}$ will allow stable laser generation. In particular, the use of FiberCore I-25 fiber with a gain parameter of $k = 0.238 \cdot 10^{-4}\,\mathrm{dB}/\mu\mathrm{m}$ and a wavelength of 45 to 65 mm demonstrated the possibility of achieving stable laser generation, and experimental work with FiberCore I-12 fiber (gain parameter $k = 0.110 \cdot 10^{-4}\,\mathrm{dB}/\mu\mathrm{m}$) and FiberCore M-12 ($k = 0.138 \cdot 10^{-4}\,\mathrm{dB}/\mu\mathrm{m}$), which highlights the importance of choosing an optical fiber to achieve the desired characteristics of a distributed feedback laser.

The experimental result showed that in a distributed feedback laser based on a 70 mm FBG, a splitting of the reflection spectrum of the FBG was observed in the FiberCore I-25 optical fiber, and at the wavelengths associated with the central wavelength of the Bragg resonance of the FBG, there was a dip in the intensity of generation associated with the capture of radiation inside the FBG at these wavelengths. This effect has been confirmed by mathematical modeling.

In recent studies on the creation of a distributed feedback laser, it has been noted that stabilization of the wavelength of laser generation is possible with the introduction of π-shift of the phase in the middle of the FBG. Our calculation shows that the introduction of the chirping effect also stabilizes the wavelength of the laser generation. The effect of small chirping $\xi = 4.3 \cdot 10^{-3}$ nm/cm is achieved with the interferometric method of recording FBG by broadcasting a laser beam along the length of the phase mask.

Funding

The research was partially supported by the Ministry of Science and Higher Education of the Russian Federation (project No. FSER-2024-0006).

Conflict of interest

The authors declare that they have no conflict of interest.

References

[1] M.I. Skvortsov. *Study of fiber lasers based on regular and random distributed feedback on structures formed by femtosecond dot recording*. Avtoref. kand. dis. (IAIE SO RAN, Novosibirsk, 2024). [Elektronnyj resurs]. URL: https://www.iae.nsk.su/images/stories/4_Education/3_DisSovet/ 250228/Avtoreferat_Skvorcov_Mihail_Igorevich.pdf

[2] I.A. Nechepurenko, A.V. Dorofeenko, O.V. Butov. Optics Express, **29** (9), 13657 (2021). DOI: 10.1364/OE.418262

[3] W. Sun, J. Shi, Y. Yu, X. Feng. Optics Continuum, **4** (2), 334 (2021). DOI: 10.1364/OSAC.414523

[4] X. Zhang, F. Zhang, Sh. Jiang, L. Min, M. Li, G. Peng, J. Ni, Ch. Wang., **7** (4), 325–328 (2017). DOI: 10.1007/s13320-017-0453-x

[5] M.I. Skvortsov, A.A. Wolf, A.A. Vlasov, K.V. Proskurina, A.V. Dostovalov, O.N. Egorova, B.I. Galagan, S. Sverchkov, B.I. Denker, S. Semjonov, S.A. Babin. Scientific Reports, **10** (1), 14487 (2020). DOI: 10.1038/s41598-020-71432-w

[6] *Specifikaciya FiberCore I-25(980/125)*. [Elektronnyj resurs]. URL: https://fibercore.humaneticsgroup.com/products/doped-fiber/erbium-doped-fiber-isogain/l-band-c-band-erbium-doped-fibers/i-25980125

[7] V. Yakimuk, S. Varzhel, I. Moor, Y.I. Yandybaeva, U. Korobkova, V. Klishina, A. Kulikov. Optik, **323**, 172216 (2025). DOI: 10.1016/j.ijleo.2025.172216

[8] Ia.D. Moor, A.V. Kulikov, D.A. Konnov, K.A. Konnov, I.A. Veremeenko, V.V. Savin. J. Optical Technology, **92** (3), 165–169 (2025). DOI: 10.1364/JOT.92.000165.

[9] *Specifikaciya FiberCore I-12(980/125)*. [Elektronnyj resurs]. URL: https://fibercore.humaneticsgroup.com/products/doped-fiber/erbium-doped-fiber-isogain/cl-band-erbium-doped-fibers/i-12980125
[10] *Specifikaciya FiberCore M-12(980/125)*. [Elektronnyj resurs]. URL: https://www.thorlabs.com/drawings/174096f82f971055-DC3EBC20-0F1B-D1C7-5918FC55A8D51D87/M12-980-125-MFGSpec.pdf
[11] R. Kashyap. *Fiber Bragg Gratings*, 2nd ed. (Academic Press, 2010).
[12] D. Marcuse. *Theory of Dielectric Optical Waveguides*, 2nd ed. (Academic Press, 1991).
[13] T. Erdogan. J. Lightwave Technology, **15**(8), 1277–1294 (1997). DOI: 10.1109/50.61832

Translated by A.Akhtyamov